



CHORUS

This is the accepted manuscript made available via CHORUS. The article has been published as:

Unified understanding of the first-order nature of the transition in math

$\text{m}_{\text{TbCo}}^{2/3}$

Chao Zhou, Tiejun Chang, Zhiyong Dai, Yuanliang Chen, Chenyang Guo, Yoshitaka Matsushita, Xiaoqin Ke, Adil Murtaza, Yin Zhang, Fanghua Tian, Wenliang Zuo, Yu-sheng Chen, Sen Yang, and Xiaobing Ren

Phys. Rev. B **106**, 064409 — Published 5 August 2022

DOI: [10.1103/PhysRevB.106.064409](https://doi.org/10.1103/PhysRevB.106.064409)

Unified understanding of the first-order nature of the transition in TbCo₂

Chao Zhou,^{1,*} Tieyan Chang,² Zhiyong Dai,¹ Yuanliang Chen,¹ Chenyang Guo,¹ Yoshitaka Matsushita,³ Xiaoqin Ke,¹ Adil Murtaza,¹ Yin Zhang,¹ Fanghua Tian,¹ Wenliang Zuo,¹ Yu-sheng Chen,² Sen Yang,^{1,†} and Xiaobing Ren⁴

¹*School of Physics, MOE Key Laboratory for Nonequilibrium Synthesis and Modulation of Condensed Matter, Xi'an Jiaotong University, Xi'an 710049, China*

²*NSF's ChemMatCARS, The University of Chicago, Lemont, IL, 60439, USA*

³*National Institute for Materials Science, Beamline BL15XU, Spring-8, 1-1-1 Kohto, Sayo-cho, Hyogo 679-5148, Japan*

⁴*Center for Functional Materials, National Institute for Materials Science, Tsukuba, Ibaraki 305-0047, Japan*

(Dated: July 21, 2022)

Determination of the nature of phase transitions, especially those that involve two symmetry-breaking order parameters, is a fundamental issue in condensed matter physics. For the Laves-phase rare-earth - transition-metal intermetallic compounds, their phase transitions involve both magnetic ordering and structural ordering. As a typical material of the Laves-phase intermetallics, TbCo₂ has been studied extensively for its transition around 230 K. However, the understanding on the nature of this transition remains controversial (first/second-order) for decades. Here in this work, based on the criteria that determine first-order and second-order transitions for magnetic materials: (1) latent heat, (2) thermal hysteresis, (3) coexistence of phases and (4) Banerjee criterion, we show direct evidence to reveal the first-order nature of the transition in TbCo₂, which is further interpreted by a Landau theory based phenomenological approach. Our work reconciles the lasting arguments on the transition of TbCo₂ and may pave the way for deepening the understanding on the transitions of magnetic materials that involve both magnetic and structural transitions.

I. INTRODUCTION

Phase transitions have been lying the foundation of magnetic functional materials, in particular the ones that involve the symmetry breaking of more than one order parameters¹. The relationship between such transitions and functionalities is well exemplified by Laves-phase rare-earth - transition-metal compounds **RT**₂ (**R** refers to rare-earth elements and **T** refers to transition-metal elements), which undergo a magnetic transition associated with a structural change².

Owing to the competition between the rare-earth - transition-metal exchange interaction and crystalline electric field effect^{3,4}, RT₂ alloys show diverse interesting effects, e.g., magnetostriction^{5,6}, magnetocaloricity^{7,8}, tunable thermal expansion⁹, magnetoresistance^{10,11}, etc. Therefore, given the direct relationship between the transition and physical properties, it is crucial to investigate the nature (first/second-order) of these phase transitions in view of both fundamental theory and application.

As one typical compound in RT₂ family, TbCo₂ has been studied extensively on both magnetic transition and structural transition around 230 K. Early studies indicate that the transition of TbCo₂ is a second-order magnetic transition associated with a structural transition¹²⁻¹⁷, which violates the common knowledge on the determination of the nature of phase transition^{18,19}. A recent study reported the first-order nature of this transition, but pointed out that the magnetic transition and structural transition decouple²⁰, contradicting with a wealth of experimental evidence^{9,21-23}. In one word, the nature of the transition in TbCo₂ remains an open question of interest.

Experimentally, for magnetic materials, the criteria

for determining second-order phase transition (**SOPT**) or first-order phase transition (**FOPT**) are: (1) latent heat^{14,24}, (2) thermal hysteresis^{14,24}, (3) phase-coexistence²⁵, and (4) Banerjee criterion²⁶⁻²⁹. In this work, based on the evidence from the above-mentioned experimental results, we show that the paramagnetic-ferrimagnetic transition in TbCo₂ is of first-order.

II. EXPERIMENTS

The TbCo₂ alloy was prepared by arc melting method with the raw materials of Tb (99.9%) and Co (99.9%) in an argon atmosphere. To ensure compositional homogeneity, the sample (about 8 g) was melted four times. The as-cast ingot was cut into slices with the thickness of 1 mm and sealed into a quartz tube, filled with argon gas; then the sealed sample was annealed at 1273 K for 72 hours, and naturally furnace-cooled to room temperature. The synchrotron X-ray diffraction (XRD) was carried out at the BL15XU NIMS beam line of Spring-8 with the X-ray wavelength $\lambda=0.6538$ Å. The samples for synchrotron XRD were well-ground powders and sealed into Kapton capillaries. The capillary was rotated during the measurement to reduce the preferred orientation effect and to average the intensity. The crystal structures were refined using the Rietveld algorithm^{30,31}. The samples used for the physical property measurements are polycrystalline bulk. The heat flow on heating and cooling processes across Curie temperature (T_C) is monitored using differential scanning calorimeter (DSC, Q2000, TA Instruments). The magnetic measurements were performed on the superconducting quantum interference device (MPMS-SQUID, Quantum Design). The magneti-

zation (M) versus temperature (T) curve was measured on cooling at the rate of 2 K/min from 260 K to 100 K, under the field of 500 Oe. The magnetic susceptibility (χ) versus temperature (T) curve was measured on cooling at the rate of 2 K/min from 260 K to 100 K, under the field 2 Oe with the frequency of 133 Hz. Before the measurement of isotherm $M(H)$ curves, magnet reset process was performed to make sure there would be no frozen field to influence the magnetization behavior at low field.

III. RESULTS AND DISCUSSION

Figure 1 shows the magnetization (M) versus temperature (T) and susceptibility (χ) versus temperature curves. From the $\partial M/\partial T$ - T (inset of Fig.1(a)) curve and fitted $1/\chi$ - T curve (inset of Fig.1(b)), deduction of the fitting can be referred to the Supplemental Material³², T_C is determined as 229.57 ± 0.01 K, agreeing well with the reported values^{9,20}.

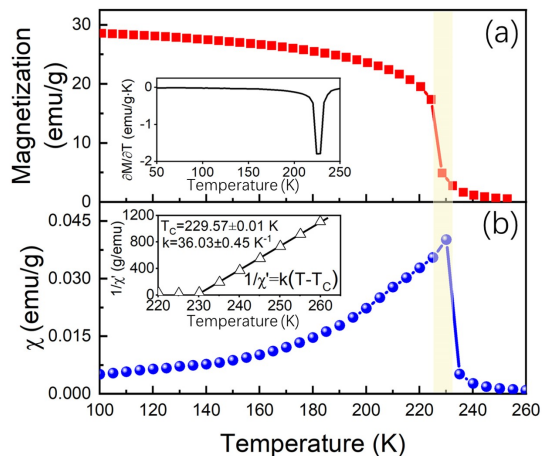


FIG. 1. (a) M - T curve and (b) χ - T curve of TbCo_2 . The derivative of magnetization over temperature and fitted $1/\chi$ - T curve are shown in the insets of (a) and (b), respectively.

The XRD profile and refined pattern at 130 K (below T_C) are shown in Fig. 2(a), and the crystallographic information is listed in Table 1. The refined XRD pattern reveals that in ferrimagnetic state, TbCo_2 crystallizes in rhombohedral structure with the space group $R\bar{3}m$ (No. 166).

The evolution of crystal structure from above T_C to below T_C , as reflected by the evolution of the characteristic reflections $\{222\}$ and $\{800\}$ from 260 K to 200 K observed from *in situ* synchrotron XRD measurements, is shown in Fig. 2(b1). At 260 K, no splitting in both $\{222\}$ and $\{800\}$ reflections is in accordance with the detected cubic crystal structure²¹. At 220 K and 200 K, the splitting in $\{222\}$ reflection and no splitting in $\{800\}$ reflection, indicate the rhombohedral crystal symmetry³³.

TABLE I. Crystal data and structure refinement for TbCo_2 at 130 K.

Wavelength	0.6538 Å		
Crystal system	Trigonal		
Space group	$R\bar{3}m$ (No. 166)		
Unit cell dimensions	a = 5.0962(1) Å		
	b = 5.0962(1) Å		
	c = 12.5336(1) Å		
	$\alpha = 90^\circ$		
	$\beta = 90^\circ$		
	$\gamma = 120^\circ$		
Volume	281.905(2) Å ³		
Goodness-of-fit on F ²	0.925		
R indices (all data)	Rp = 6.62%	Rwp = 9.34%	
Atomic parameters			
Atom	Wyckoff Position	Occ.	
Tb	6c	0,0,0.1243	1
Co1	3b	0,0,0.5	1
Co2	9e	0.5,0,0	1

At 230 K, which is the detected magnetic transition temperature from M - T curve (Fig. 1(a)) and χ - T curve (Fig. 1(b)), the asymmetric peak shape of the reflections $\{222\}$ and $\{800\}$, especially of $\{800\}$, is observed clearly, which indicates the phase-coexistence state. Besides, the asymmetric peaks are consistent with the superposition of cubic and rhombohedral profiles. Further on cooling, the emergent splitting of $\{222\}$ reflection below T_C unambiguously suggests a structure phase transition, and the observed phase coexistence at 230 K further proves the first-order nature of the transition. The calculated lattice parameters and spontaneous lattice strain ε (the calculation of ε can be referred to Ref.²⁵) are shown in Fig.2(b2).

The DSC measurement was carried out to check the heat flow during transition (Fig. 3). The appearance of exothermic peak on cooling process and the endothermic peak on heating process, proves FOPT around 230 K. The temperatures of exothermic peak and endothermic peak are 228 K and 233 K (at the rate of 6 K/min), respectively, agreeing well with the magnetic transition temperature (Fig.1). To eliminate the impact of temperature ramp rate, the rate-dependence (2, 4, 6, 8, 10, 12, 14 K/min) of measured peak temperatures is investigated and presented in the inset of Fig.3. Following the common treatment^{34,35}, linear fitting is adopted to fit the rate-dependence. The magnitude of the thermal hysteresis approximates to ~ 1 K at an extrapolated zero ramp rate, comparable to the value reported recently (0.6 K)²⁰. The non-zero latent heat (DSC peak) and the thermal hysteresis both reveal the first-order nature of the transition around 230 K. It should be noted that the thermal hysteresis between exothermic and endothermic peaks was previously detected but neglected, and thus

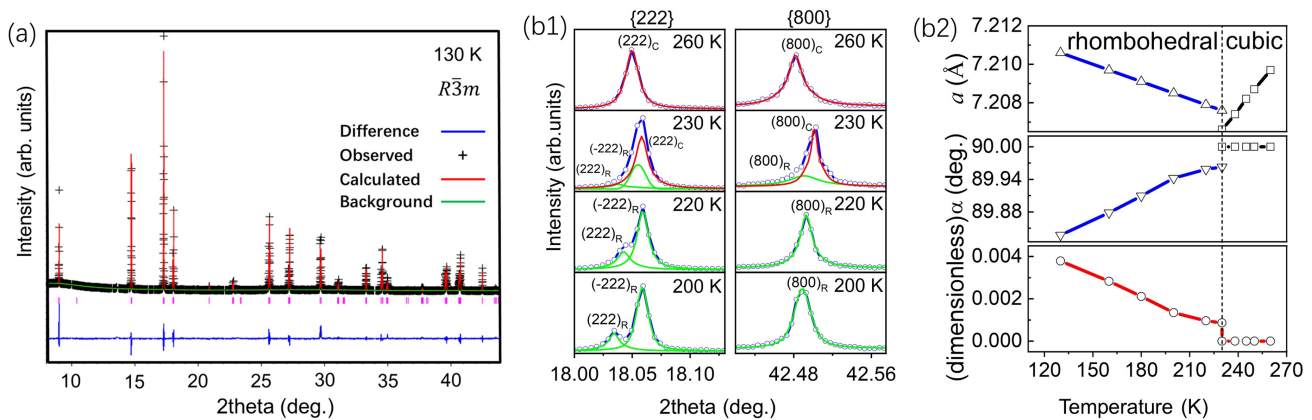


FIG. 2. (a) The refined XRD patterns for TbCo_2 at 130 K. The background and calculated Bragg peaks positions are shown below the observed (plus) and calculated (red line) intensities, and the difference is shown by blue line at the bottom; (b1) the characteristic XRD reflections $\{222\}$ and $\{800\}$ at 260 K, 230 K, 220 K and 200 K, respectively, with the red, green and blue lines denoting the cubic fit, rhombohedral fits and full sum, respectively; (b2) the lattice parameters and lattice strain within the temperature range 130 K~260 K.

the transition at ~ 230 K was incorrectly classified as second-order magnetic transition associated with a structural change¹³.

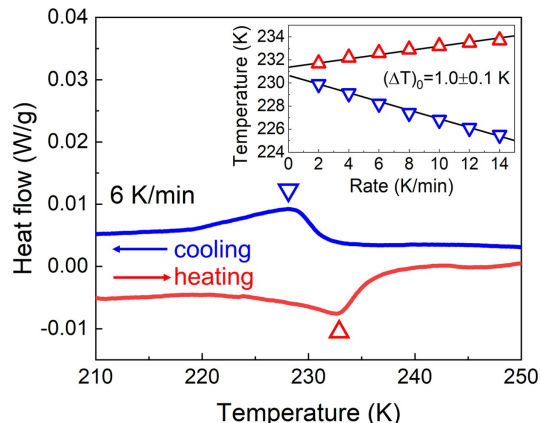


FIG. 3. Heat flow of TbCo_2 on heating and cooling processes at the rate of 6 K/min. The inset shows the ramp rate dependence (linear fitting) of exothermic and endothermic peak temperatures.

Since that the transition in TbCo_2 has been regarded second-order for long, the theoretical models for SOPT, i.e., scaling hypothesis and Heisenberg model¹³, were employed for investigating the transition. Here in this work, the nature of transition of TbCo_2 is analyzed from the Arrott-plots method following the Banerjee criterion²⁶.

Fig.4 shows the magnetization isotherms and the corresponding Arrott plots ($H/M - M^2$) within the temperature range across T_C . From Fig.4(a), it is seen that the change of magnetization from neighboring temperatures reaches the maximum at 230 K. The negative slopes of $H/M - M^2$ curves are observed in Fig.4(b), demonstrating

the FOPT according to Banerjee's criterion^{36,37}. Attention should be paid to that the negative slopes appear in the low magnetization region (inset of Fig.4(b)), where the data points might be missed if the measurement step of H is not small enough. And this may explain why the Arrott-plots method was used for TbCo_2 but the negative slopes were not observed^{13,21,38}.

An interesting fact is that, many of the previously reported "SOPT" of magnetic materials have been revised to FOPT in recent years, e.g. Fe, Ni, Co, CoFe_2O_4 , NdCo_2 and PrCo_2 ^{14,24,39}. This is not difficult to understand, as we will show in the following by using a Landau phenomenological approach.

Under an applied magnetic field, the change in Gibbs free energy per unit of volume (See Equ.(S1) in the Supplemental Material³²) is modified as⁴⁰:

$$\Delta G(M, H) = \frac{1}{2}a_0(T - T_C)M^2 + \frac{1}{4}bM^4 + \frac{1}{6}cM^6 - M \cdot H \quad (1)$$

where H is the applied magnetic field.

The equilibrium condition $\partial \Delta G(M, H) / \partial M = 0$ leads to:

$$H = a_0(T - T_C)M + bM^3 + cM^5 \quad (2)$$

Therefore, H and M follows the nonlinear relationship as Equ.(2) expresses. From the fitted curve (Fig.5(a)), the value of b is calculated to be 1.965×10^{-17} ($\text{J} \cdot \text{m} / \text{A}^4$).

For the materials that the structural transition and the magnetic transition occur synchronously, strong coupling exists between the two order parameters of magnetization (primary) and lattice strain (secondary)²⁵, as demonstrated in the case of TbCo_2 ⁴¹. Then, the change of Gibbs free energy is rewritten as^{24,25}:

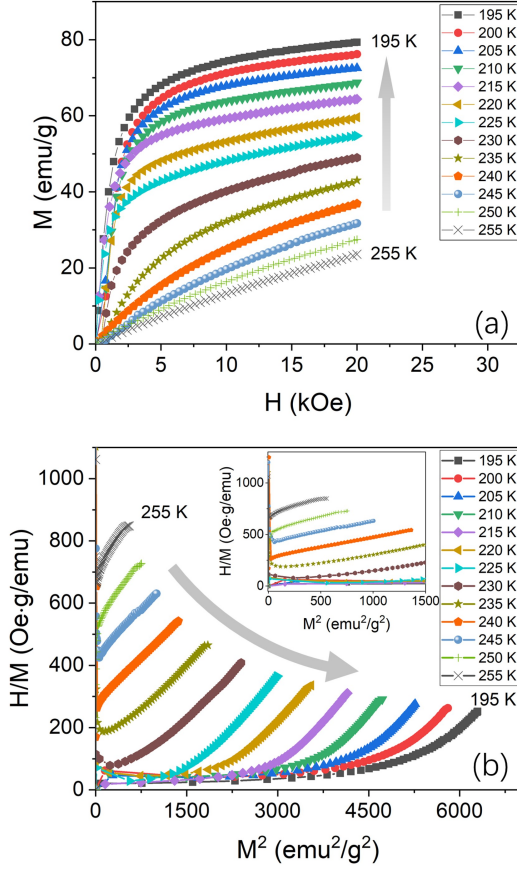


FIG. 4. (a) The magnetization isotherms measured at selected temperatures near T_C under the applied field of 2 Tesla; (b) the isotherms of $H/M-M^2$, the inset shows the curve of low magnetization region.

$$\Delta G(M, \varepsilon) = \frac{1}{2}a_0(T - T_C)M^2 + \frac{1}{4}bM^4 + \frac{1}{6}cM^6 + \frac{1}{2}K\varepsilon^2 + \lambda\varepsilon \cdot M^2 \quad (3)$$

where the elastic energy ($\frac{1}{2}K\varepsilon^2$) and the magnetoelastic coupling energy ($\lambda\varepsilon \cdot M^2$) are added, in which K is the elastic modulus, ε is the lattice strain and λ is the coupling coefficient.

Minimizing the energy with respect to the strain ($\partial\Delta G(M, \varepsilon)/\partial\varepsilon = 0$) yields a relation between ε and M^2 :

$$\varepsilon = -\frac{\lambda}{K}M^2 \quad (4)$$

Substituting Equ.(4) into Equ.(3) leads to:

$$\Delta G = \frac{1}{2}a_0(T - T_C)M^2 + \left(\frac{1}{4}b - \frac{\lambda^2}{2K}\right)M^4 + \frac{1}{6}cM^6 \quad (5)$$

Therefore, the order of the transition can be determined from the value of the coefficient of the fourth-order term ($\frac{b}{4} - \frac{\lambda^2}{2K}$)²⁸.

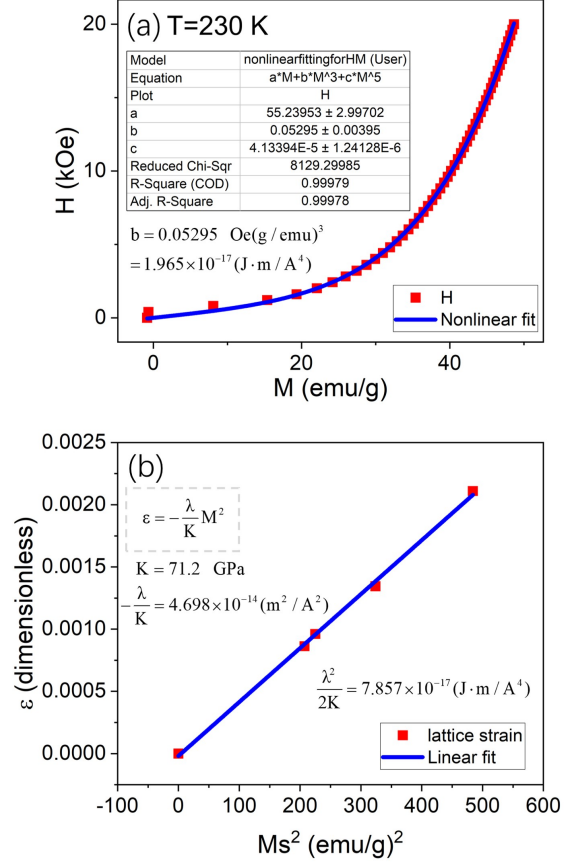


FIG. 5. (a) H versus M curve and nonlinear fitting, (b) lattice strain ε versus M^2 and linear fitting. In Fig.5(b), the values of M and ε are obtained from $M-H$ loops and the synchrotron XRD patterns measured at 180 K, 200 K, 220 K and 230 K; the value of K (71.2 GPa) is taken from Ref.²⁰.

Based on the spontaneous magnetization (M_s , calculated using the law of approach to saturation (LAS)^{42,43}) and lattice strain (ε , calculated from the XRD patterns (Fig.2(b2))), the linear relation $\varepsilon \sim Ms^2$ is fitted as shown in Fig.5(b). The value of $\lambda^2/2K$ is calculated to be 7.857×10^{-17} ($J \cdot m/A^4$). As a result, the coefficient of the fourth-order term $\frac{b}{4} - \frac{\lambda^2}{2K} = -7.366 \times 10^{-17}$ ($J \cdot m/A^4$), is small but indeed negative, suggesting the weak FOPT⁴⁴. Such conclusion is consistent with that obtained from Figs.1-4.

Last but not least, it should be pointed out that the coupling of magnetization with the lattice strain, which results from the exchange interaction effect⁴⁵, would drive the magnetic ordering to become first-order^{2,46,47}. If the exchange interaction is admitted being a function of lattice inter-atomic spacing and the lattice is deformable, then the transition would become FOPT, and yield latent heat as well as a spontaneous lattice strain at the transition point^{48,49}. Again, we suggest the scarcity of purely second-order ferro(ferri)-magnetic transition, as long as the inevitable coupling between the magnetization and the crystal lattice exists²⁴.

IV. CONCLUSION

In conclusion, from the detected thermal hysteresis, latent heat, structural transition and Banerjee criterion, we show that the transition of TbCo₂ around 230 K is FOPT, which can be well understood based on Landau theory model. Moreover, our findings unifies the understanding on the transition of TbCo₂: FOPT with synchronous first-order structural transition and first-order ferrimagnetic transition. Our work may provide an insight into investigating the nature of other alleged second-order transitions for the magnetic materials that undergo both magnetic and structural transitions.

ACKNOWLEDGMENTS

The authors are grateful to Qizhong Zhao, Kang Cao and Ruisheng Zhang for experimental assistance. This work was financially supported by the National Key R & D Program of China (2021YFB3501401), the National Natural Science Foundation of China (Grants Nos. 91963111, 51601140), Key Scientific and Technological Innovation Team of Shaanxi Province (2020TD001), Innovation Capability Support Program of Shaanxi (Nos. 2018PT-28, 2017KTPT-04). NSF's ChemMatCARS Sector 15 is supported by the Divisions of Chemistry (CHE) and Materials Research (DMR), National Science Foundation, under grant number NSF/CHE-1834750.

-
- * chao.zhou@xjtu.edu.cn
 † yang.sen@xjtu.edu.cn
- ¹ M. M. Vopson, *Critical Reviews in Solid State and Materials Sciences* **40**, 223 (2015).
 - ² S. L. Driver, J. Herrero-Albillos, C. M. Bonilla, F. Bartolome, L. M. Garcia, C. J. Howard, and M. A. Carpenter, *Journal of Physics-Condensed Matter* **26**, 056001 (2014).
 - ³ A. E. Clark and H. S. Belson, *Physical Review B* **5**, 3642 (1972).
 - ⁴ J. J. Melero and R. Burriel, *Journal of Magnetism and Magnetic Materials* **157-158**, 651 (1996).
 - ⁵ A. E. Clark, J. R. Cullen, O. D. McMasters, and E. R. Callen, *AIP Conference Proceedings* **29**, 192 (1976).
 - ⁶ S. Yang, H. Bao, C. Zhou, Y. Wang, X. Ren, Y. Matsushita, Y. Katsuya, M. Tanaka, K. Kobayashi, X. Song, and J. Gao, *Physical Review Letters* **104**, 197201 (2010).
 - ⁷ E. Z. Valiev, *Journal of Experimental and Theoretical Physics* **124**, 968 (2017).
 - ⁸ K. Gu, J. Li, W. Ao, Y. Jian, and J. Tang, *Journal of Alloys and Compounds* **441**, 39 (2007).
 - ⁹ Y. Song, J. Chen, X. Liu, C. Wang, J. Zhang, H. Liu, H. Zhu, L. Hu, K. Lin, S. Zhang, and X. Xing, *Journal of the American Chemical Society* **140**, 602 (2018).
 - ¹⁰ J. A. Chelvane, G. Markandeyulu, N. H. Kumar, R. Nir-mala, and S. K. Malik, *Physical Review B* **72**, 092406 (2005).
 - ¹¹ S. Radha, S. B. Roy, A. K. Nigam, and G. Chandra, *Physical Review B* **50**, 6866 (1994).
 - ¹² E. W. Lee and F. Pourarian, *Physica Status Solidi a-Applied Research* **33**, 483 (1976).
 - ¹³ M. Halder, S. M. Yusuf, M. D. Mukadam, and K. Shashikala, *Physical Review B* **81**, 174402 (2010).
 - ¹⁴ J. Herrero-Albillos, F. Bartolome, L. M. Garcia, F. Casanova, A. Labarta, and X. Batlle, *Physical Review B* **73**, 134410 (2006).
 - ¹⁵ S. Khmelevskiy and P. Mohn, *Journal of Physics-Condensed Matter* **12**, 9453 (2000).
 - ¹⁶ E. Gratz and H. Sassik, *Journal of Physics F: Metal Physics* **11**, 429 (1981).
 - ¹⁷ C. M. Bonilla, J. Herrero-Albillos, F. Bartolome, L. M. Garcia, M. Parra-Borderias, and V. Franco, *Physical Review B* **81**, 224424 (2010).
 - ¹⁸ S. Yang, H. Bao, C. Zhou, Y. Wang, X. Ren, X. Song, Y. Matsushita, Y. Katsuya, M. Tanaka, and K. Kobayashi, *Chinese Physics B* **22**, 046101 (2013).
 - ¹⁹ S. B. Roy, *Journal of Physics-Condensed Matter* **25**, 183201 (2013).
 - ²⁰ D. Huang, J. Gao, S. H. Lapidus, D. E. Brown, and Y. Ren, *Materials Research Letters* **8**, 97 (2020).
 - ²¹ C. Fang, J. Wang, F. Hong, W. D. Hutchison, M. F. M. Din, A. J. Studer, J. A. Kimpton, S. Dou, and Z. Cheng, *Physical Review B* **96**, 064425 (2017).
 - ²² N. Yoshimoto, J. Sakurai, and Y. Komura, *Journal of Magnetism and Magnetic Materials* **31-34**, 137 (1983).
 - ²³ Z. W. Ouyang, F. W. Wang, Q. Hang, W. F. Liu, G. Y. Liu, J. W. Lynn, J. K. Liang, and G. H. Rao, *Journal of Alloys and Compounds* **390**, 21 (2005).
 - ²⁴ S. Yang, X. Ren, and X. Song, *Physical Review B* **78**, 174427 (2008).
 - ²⁵ S. Yang and X. Ren, *Physical Review B* **77**, 014407 (2008).
 - ²⁶ S. K. Banerjee, *Physics Letters* **12**, 16 (1964).
 - ²⁷ X. Zhou, W. Li, H. P. Kunkel, and G. Williams, *Physical Review B* **73**, 012412 (2006).
 - ²⁸ M. Parra-Borderias, F. Bartolome, J. Herrero-Albillos, and L. M. Garcia, *Journal of Alloys and Compounds* **481**, 48 (2009).
 - ²⁹ M. Hsini and L. Ghivelder, *Physica B: Condensed Matter* **615**, 413055 (2021).
 - ³⁰ H. M. Rietveld, *Journal of applied Crystallography* **2**, 65 (1969).
 - ³¹ R. Young, *The Rietveld Method* (Oxford University Press, Oxford, 1993).
 - ³² See Supplemental Material at [URL will be inserted by publisher] for the deduction of the linear relation between the reciprocal susceptibility and temperature.
 - ³³ T. Y. Chang, C. Zhou, J. W. Mi, K. Y. Chen, F. H. Tian, Y. S. Chen, S. G. Wang, Y. Ren, D. E. Brown, X. P. Song, and S. Yang, *Journal of Physics-Condensed Matter* **32**, 135802 (2020).
 - ³⁴ S. Brooker, *Chemical Society Reviews* **44**, 2880 (2015).
 - ³⁵ T.-H. Hsu, C.-H. Chung, F.-J. Chung, C.-C. Chang, M.-C. Lu, and Y.-L. Chueh, *Nano Energy* **51**, 563 (2018).
 - ³⁶ J. Y. Law, V. Franco, L. M. Moreno-Ramrez, A. Conde, D. Y. Karpenkov, I. Radulov, K. P. Skokov, and O. Gut-fleisch, *Nature Communications* **9**, 2680 (2018).
 - ³⁷ D. Guo, L. M. Moreno-Ramrez, C. Romero-Muniz, Y. Zhang, J.-Y. Law, V. Franco, J. Wang, and Z. Ren, *Science China Materials* **64**, 2846 (2021).

- ³⁸ N. K. Singh, K. G. Suresh, A. K. Nigam, S. K. Malik, A. A. Coelho, and S. Gama, *Journal of Magnetism and Magnetic Materials* **317**, 68 (2007).
- ³⁹ M. Forker, S. Muller, P. dela Presa, and A. F. Pasquevich, *Physical Review B* **75**, 187401 (2007).
- ⁴⁰ N. H. van Dijk, *Journal of Magnetism and Magnetic Materials* **529**, 167871 (2021).
- ⁴¹ D. Gignoux, F. Givord, and F. Sayetat, *Journal of Magnetism and Magnetic Materials* **15-18**, 1235 (1980).
- ⁴² M. Vazquez, W. Fernengel, and H. Kronmller, *Physica Status Solidi (a)* **115**, 547 (1989).
- ⁴³ A. M. Alsmadi, I. Bsoul, S. H. Mahmood, G. Alnawashi, K. Prokes, K. Siemensmeyer, B. Klemke, and H. Nakotte, *Journal of Applied Physics* **114**, 243910 (2013).
- ⁴⁴ K. Morrison, A. Dupas, Y. Mudryk, V. K. Pecharsky, K. A. Gschneidner, A. D. Caplin, and L. F. Cohen, *Physical Review B* **87**, 134421 (2013).
- ⁴⁵ S. Bustingorry, F. Pomiro, G. Aurelio, and J. Curiale, *Physical Review B* **93**, 224429 (2016).
- ⁴⁶ J. Inoue and M. Shimizu, *Journal of Physics F: Metal Physics* **18**, 2487 (1988).
- ⁴⁷ N. Duc, P. Brommer, and J. Franse, *Physica B: Condensed Matter* **191**, 239 (1993).
- ⁴⁸ C. P. Bean and D. S. Rodbell, *Physical Review* **126**, 104 (1962).
- ⁴⁹ O. Rice, *The Journal of Chemical Physics* **22**, 1535 (1954).